Title

Regenerating Corticospinal Axons Innervate Phenotypically Appropriate Neurons within Neural Stem Cell Grafts

Journal

Cell Reports, 26(9)

ISSN

2639-1856

Authors

Kumamaru, Hiromi

Lu, Paul

Rosenzweig, Ephron S

et al.

Publication Date

2019-02-01

DOI

10.1016/j.celrep.2019.01.099

HHS Public Access

Author manuscript

Cell Rep. Author manuscript; available in PMC 2019 April 29.

Published in final edited form as:

Cell Rep. 2019 February 26; 26(9): 2329–2339.e4. doi:10.1016/j.celrep.2019.01.099.

Regenerating Corticospinal Axons Innervate Phenotypically Appropriate Neurons within Neural Stem Cell Grafts

Hiromi Kumamaru[1,2], **Paul Lu**[1,3], **Ephron S. Rosenzweig**[1], **Ken Kadoya**[1,4], and **Mark H. Tuszynski**[1,3,5,*]

[1]Department of Neurosciences, University of California, San Diego, La Jolla, CA, USA

[2]Department of Orthopaedic Surgery, Kyushu University Beppu Hospital, Oita, Japan

[3]Veterans Administration San Diego Healthcare System, San Diego, CA, USA

[4]Department of Orthopaedic Surgery, Hokkaido University, Sapporo, Japan

[5]Lead Contact

SUMMARY

Neural progenitor cell grafts form new relays across sites of spinal cord injury (SCI). Using a panel of neuronal markers, we demonstrate that spinal neural progenitor grafts to sites of rodent SCI adopt diverse spinal motor and sensory interneuronal fates, representing most neuronal subtypes of the intact spinal cord, and spontaneously segregate into domains of distinct cell clusters. Host corticospinal motor axons regenerating into neural progenitor grafts innervate appropriate pre-motor interneurons, based on *trans*-synaptic tracing with herpes simplex virus. A human spinal neural progenitor cell graft to a non-human primate also received topographically appropriate corticospinal axon regeneration. Thus, grafted spinal neural progenitor cells give rise to a variety of neuronal progeny that are typical of the normal spinal cord; remarkably, regenerating injured adult corticospinal motor axons spontaneously locate appropriate motor domains in the heterogeneous, developing graft environment, without a need for additional exogenous guidance.

Graphical Abstract

*Correspondence: mtuszynski@ucsd.edu.

AUTHOR CONTRIBUTIONS

H.K. designed and carried out experiments, interpreted results, and wrote the manuscript. P.L. contributed to CST tracing experiments. E.S.R. contributed to the human cell graft experiment. K.K. contributed to the conception of the project. M.H.T. contributed to the conception of the project, interpretation of results, and wrote the manuscript.

SUPPLEMENTAL INFORMATION

Supplemental Information can be found with this article online at https://doi.org/10.1016/j.celrep.2019.01.099.

DECLARATION OF INTERESTS

The authors declare no competing interests.

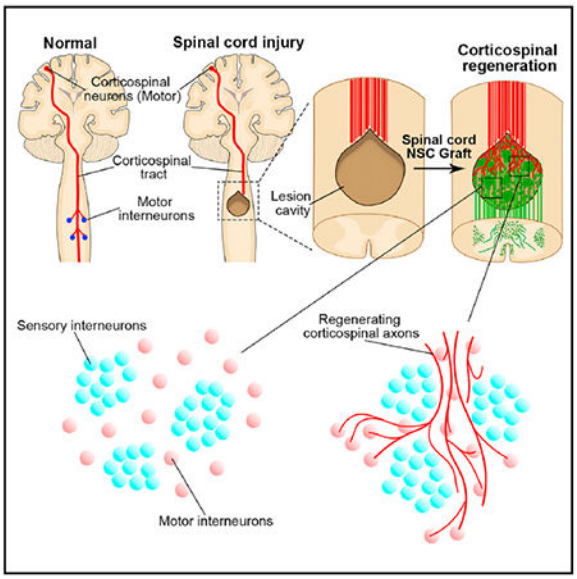

In Brief

Kumamaru et al. demonstrate that spinal cord neural progenitor cell grafts spontaneously segregate into motor and sensory domains when implanted into sites of spinal cord injury in rats and primates. Host corticospinal axons regenerating into grafts preferentially regenerate and synapse onto motor interneuron-rich domains, avoiding inappropriate sensory domains.

INTRODUCTION

Grafts of neural stem cells to the injured spinal cord have recently been shown to extend very large numbers of axons into degenerating white matter tracts of the injured spinal cord (Kadoya et al., 2016; Kumamaru et al., 2018; Lu et al., 2012, 2014; Rosenzweig et al., 2018), and host axons, in turn, regenerate into the developing milieu of the graft (Dulin et al., 2018; Kadoya et al., 2016; Lu et al., 2012; Medalha et al., 2014; Rosenzweig et al., 2018). Regenerating host axons form synapses in the graft (Adler etal.,2017; Kadoya et al., 2016; Kumamaru et al., 2018; Lu et al., 2012; O'Shea et al., 2017)., and graft-derived axons form synapses in host gray matter caudal to the lesion site (Kadoya et al., 2016; Lu et al., 2012). Synaptic transmission across the lesion is partially restored (Lu et al., 2012), and functional deficits improve (Curtis et al., 2018; Kadoya et al., 2016; Kumamaru et al., 2018; Lu et al., 2017; Rosenzweig et al., 2018), even after complete spinal cord transection (Lu et al., 2012).

These intriguing findings raise important mechanistic questions; prominent among these is whether *host* axons regenerating into neural progenitor cell grafts contact appropriate synaptic partners in the graft (Hilton and Bradke, 2017) or whether exogenous guidance to appropriate partners is required to optimize graft functional connectivity. We recently reported that regenerating host sensory axons arising from dorsal root ganglion neurons project to appropriate, calretinin-expressing, sensory, neuronal target domains within neural progenitor cell grafts (Dulin et al., 2018). However, the topography of motor axonal

projections into neural progenitor cell grafts, and whether they contact phenotypically appropriate target neurons within the grafts, has not been established; this is an especially important question to address for the corticospinal projection, the most important voluntary motor-control system in humans. Indeed, to date, phenotypic characterization of the fates of neural progenitor cells grafted to sites of spinal cord injury (SCI) has not been performed in detail, other than the use of general neuronal markers, such as neuronal nuclei (NeuN) or doublecortin (DCX) and broad excitatory or inhibitory neuronal markers (Guo et al., 2010; Yan et al., 2007). Thus, the neuronal subtype fates of grafted cells remain unknown.

Recent advances have made a variety of tools available to address these questions. Studies of spinal cord development have provided panels of transcriptional and other neuron-specific markers that have identified more than 20 subtypes of interneurons in the spinal cord (Alaynick et al., 2011; Arber, 2012; Goulding, 2009; Kiehn, 2016; Lai et al., 2016; Levine et al., 2014; Sathyamurthy et al., 2018). Each neuronal subtype has a specific functional role (Bikoff et al., 2016; Lu et al., 2015) through the formation of local networks with highly selective synaptic inputs and outputs (Goulding, 2009; Lu et al., 2015). For example, excitatory interneuronal V2a subsets exert a key role in coordinating and maintaining locomotor rhythmicity and are labeled by Chx10 (Azim et al., 2014; Dougherty and Kiehn, 2010). A V1 inhibitory motor neuronal subset exerts a major role in shaping spinal motor output and is labeled by FoxP2 (Bikoff et al., 2016). Recently, direct connectivity between motor corticospinal neurons and these spinal pre-motor neurons (e.g., Chx10-expressing V2a, Chat-expressing V0c, or En1-expressing V1 neurons) were identified in the rodent spinal cord (Ueno et al., 2018). Motor synergy encoder (MSE) neurons, which are labeled by Ap2b and Satb1, also receive direct input from corticospinal neurons and extend monosynaptic outputs to spinal motor neurons (Levine et al., 2014), comprising a cellular network for encoding coordinated motor output programs (Levine et al., 2014). In addition, new *trans*-synaptic tracing tools provide the opportunity to identify synaptic partners of host motor axons, such as corticospinal axons regenerating into grafts, using anterograde *trans*-synaptic tracing with the H129 strain of herpes simplex virus 1 (HSV) (Lo and Anderson, 2011; Wojaczynski et al., 2015).

Using these tools, we now find that neural progenitor cell grafts self-assemble into distinct pre-motor and sensory domains after grafting into sites of SCI. Importantly, regenerating adult corticospinal axons preferentially synapse onto appropriate pre-motor neuronal partners that recapitulate patterns of the corticospinal projection in the intact spinal cord (Levine et al., 2014; Ueno et al., 2018), including synaptic connectivity with Chx10, Ap2b, Satb1, FoxP2, and ChAT-expressing neurons. The provision of exogenous *guidance* to regenerating host corticospinal axons toward appropriate neuronal targets within grafts may not be necessary, potentially simplifying the clinical translation of neural stem cell therapies for spinal cord injury.

RESULTS

Grafts to Rodent Models

Phenotypic Characterization of Spinal Cord Neural Progenitor Cell-Derived Neurons—We first systematically characterized the fates of rat embryonic day 14 (E14)

spinal cord-derived neural progenitor cell grafts using a panel of transcription factors that are restricted to specific neuronal subsets (Alaynick et al., 2011; Del Barrio et al., 2013; Lu et al., 2015). Neural progenitor cell grafts expressed GFP under the ubiquitin promoter, enabling clear characterization of grafted cells. Rats underwent bilateral C4 dorsal spinal cord lesions, followed by immediate placement of cell grafts into lesion sites (n = 8 animals). Four rats were sacrificed 2 weeks later, an early time point at which several neuronal developmental transcriptional neuronal markers are expressed (but are subsequently downregulated), and four rats were sacrificed after 6 months when mature neuronal markers are fully expressed.

Two weeks after grafting, cells expressed the immature neuronal marker DCX and the more mature neuronal marker, NeuN (Figures 1A and 1B). Grafted neurons also expressed the general motor neuronal marker Isl1/2 (Figure 1C) and the intermediate-ventral interneuronal markers Bhlhb5 or Prdm8 (Figures 1D and 1E) (Lai et al., 2016; Lu et al., 2015). The intermediate-ventral neurons were further identified into pre-motor subgroups of Chx10-excitatory V2a interneurons (Figure 1F) or FoxP2-inhibitory V1 interneurons (Figure 1G). Lhx3- or FoxP1-expressing interneurons were also observed at this phase (Figures S1A and S1B). Grafted neurons also expressed the spinal somatosensory interneuronal markers Brn3a (somatosensory relay neurons, dl1-3, dlL_B, and dl5; Figure 1H) (Gross et al., 2002; Müller et al., 2002), Lbx1 (somatosensory association neurons, dl4-6; Figure 1I) (Gross et al., 2002; Müller et al., 2002), or Tlx3 (excitatory somatosensory neurons, dl3, dlL_B, and dl5; Figure 1J) (Cheng et al., 2004; Xu et al., 2008) and the inhibitory interneuronal marker Pax2 (Figure 1K) (Cheng et al., 2004). We refer to spinal somatosensory neurons as “sensory interneurons” in this study (Mizuguchi et al., 2006). Quantification of these transcription factor-expressing neurons 2 weeks after grafting revealed that most grafted neural progenitor cells expressed sensory interneuronal markers: 73.6% ± 7.1% of grafted neurons co-labeled with NeuN and sensory interneuronal markers (Brn3a, Lbx1, orTlx3; Figure 1L; see STAR Methods). This finding is consistent with donor cells obtained from the E14 rat spinal cord predominantly expressing the dorsal progenitor marker Pax7 (dl1-6; Figures S1C) (Alaynick et al., 2011; Lai et al., 2016); fewer E14 spinal cord cells express the ventral progenitor markers Nkx6.1 and Nkx2.2 (Figures S1D and S1E) (Alaynick et al., 2011) or the motor neuron progenitor marker Olig2 (Figure S1E) (Alaynick et al., 2011). Two weeks after grafting, only 19.0% ± 2.1% of grafted cells expressed the inhibitory interneuronal marker Pax2 (Figures 1K and 1L).

When examined 6 months after implantation, grafts had differentiated into fully mature neurons ($NeuN^+/DCX^-$) and expressed several mature neuronal markers. Of cells expressing neuronal markers at 6 months, 70.1% ± 4.7% expressed calmodulin-dependent protein kinase II (CaMKII), which is expressed by excitatory neurons (Figures 1M and 1P). Cells also expressed choline acetyltransferase (ChAT; Figure 1N) for cholinergic motor and V0c interneurons or GABA (Figure 1O) for inhibitory neurons. At 6 months, we were not able to use many of the cell type-specific transcription factor markers (Prdm8, Bhlhb5, Pax2, and Isl1/2) employed at 2 weeks after grafting because these are downregulated in mature neurons. We did not quantify mature sensory interneuronal markers because most of them (e.g., calbindin, calretinin, and parvalbumin) are not expressed exclusively by spinal sensory

interneurons and are used in conjunction with neuronal location in intact dorsal spinal gray matter to identify sensory interneurons (Alvarez et al., 2005).

Combining findings from 2-week and 6-month studies, we find that, overall, spinal cord neural progenitor cell grafts predominantly adopt an excitatory neuronal fate and express a diverse set of pre-motor and sensory interneuronal markers.

Spatial Distribution of Graft Neuronal Subtypes—We next assessed the spatial distribution of neuronal subtypes within grafts of GFP-negative E14 donor grafts (n = 4) 2 weeks after implantation. Cells expressing the motor neuronal marker Isl1/2 and the pre-motor interneuronal markers Prdm8, Chx10, FoxP1, and FoxP2 were sparsely distributed throughout grafts (Figures 2A, 2B, and S2A-S2F); intercalated on that background of pre-motor interneuronal cells were distinct and dense cell clusters expressing spinal sensory interneuronal markers (e.g., Tlx3; Figures 2C-2H and S2A). Thus, pre-motor populations exist in distinct domains separate from sensory interneuronal domains. Pax2-expressing inhibitory interneurons were uniformly distributed within both motor and sensory domains (Figure 2I). Within sensory interneuronal clusters, a variety of spinal sensory interneuronal subtypes were expressed, including Tlx3, Lbx1, and Brn3a (Figure 2C), consistent with a recent report (Dulin et al., 2018). Six months after implantation, grafts also exhibited spontaneous organization into distributed motor domains (ChAT, Chx10, or FoxP2 expressing motor or pre-motor neurons) with interspersed, separated clusters of Tlx3-expressing sensory interneurons (Figures S2G-S2I and S3). Thus, the cardinal motor and sensory domains of the spinal cord are represented in neural progenitor cell grafts (Figure 2J). In the present study, rat neural progenitor cells were grafted into the dorsal columns, a white matter structure that is normally devoid of neurons. Thus, NeuN-expressing cells observed in the dorsal columns are exclusively graft derived, and we assessed findings only among NeuN-expressing cells exclusively located in white matter.

Corticospinal Axons Preferentially Regenerate into Motor Interneuronal Graft Domains—We previously reported that corticospinal axons regenerate into neural progenitor cell grafts in sites of spinal cord injury (Kadoya et al., 2016; Kumamaru et al., 2018), but we do not know whether those corticospinal axons synapse onto phenotypically appropriate or inappropriate target neurons in grafts (Hilton and Bradke, 2017). Using a toolbox consisting of the neuronal fate-specific markers reported above together with anterograde *trans*-synaptic herpes virus (HSV129) tracing (Lo and Anderson, 2011; Wojaczynski et al., 2015), we investigated the new synaptic partners of lesioned adult corticospinal axons growing into neural progenitor cell grafts.

In the first experiment, we injected AAV8 vectors expressing membrane-targeted tdTomato into bilateral motor cortices to anterogradely label corticospinal axons (n = 4). E14-derived spinal cord neural progenitor cells were grafted into C4 spinal cord dorsal column lesion sites 2 weeks later. Two weeks after grafting, animals were sacrificed. TdTomato-labeled corticospinal axons grew into graft neuronal domains expressing Prdm8, a marker of V0-2 interneurons (Figures 3A and 3C) (Francius et al., 2013; Lu et al., 2015), and avoided sensory neuronal islands expressing Tlx3 (Figures 3B and 3D) (Alaynick et al., 2011; Cheng et al., 2004; Xu et al., 2008). Indeed, 84.1% ± 3.2% of corticospinal axons growing into

grafts were present in these distinct motor interneuronal domains that were separate from Tlx3-expressing sensory neuronal clusters. There is no corticospinal regeneration into empty lesion cavities or into lesion cavities containing bone marrow stromal cell grafts or Schwann cell grafts (Kadoya et al., 2016).

The preferential innervation of motor interneuronal domains persisted when grafts were examined 6 months after grafting (n = 4): indeed, 90.8% ± 2.0% of corticospinal axons in grafts were present in these distinct interneuronal domains that were separate from Tlx3-expressing sensory neuronal clusters (Figures 3E and 3F). At that time, Prdm8 had undergone developmental downregulation and could no longer be detected. These results reveal that corticospinal fibers preferentially grow into motor interneuron-rich domains within neural progenitor grafts (Figure 2J).

In the second experiment, we identified synaptic partners of growing corticospinal axons within distinct graft neuronal domains using a Cre-dependent anterograde poly-*trans*-synaptic H129 herpes simplex virus (HSV) (Lo and Anderson, 2011; Wojaczynski et al., 2015). Six intact animals received cortical injections of AAV9-Cre, together with AAV8-GFP, into the primary motor cortex (see STAR Methods); four additional animals received injections of AAV8-GFP only into the primary motor cortex, without accompanying AAV9-Cre injections. Two weeks later, all animals underwent C4 dorsal column lesions, to transect the main corticospinal projection bilaterally, and received grafts of E14-derived spinal cord neural progenitor cells into the lesion site. Two weeks after grafting, animals received injections of Cre-dependent HSV-H129ΔTK-tdTomato into the motor cortex, initiating HSV-tdTomato *trans*-synaptic spread. One and 2 days after cortical injections of Cre-HSV-tdTomato, animals did not exhibit labeling of neurons in grafts (Lo and Anderson, 2011; Wojaczynski et al., 2015), whereas animals sacrificed 3 days after cortical injections of Cre-HSV-tdTomato *did* exhibit tdTomato-labeled neurons in grafts (Figures 4A and 4B). Thus, sacrifice of animals 3 days after cortical Cre-HSV-tdTomato injections likely labeled the primary, and possibly secondary, post-synaptic partners of corticospinal neurons. Notably, graft neurons *trans*-synaptically labeled with tdTomato 3 days after Cre-HSV-tdTomato into the motor cortex expressed *motor* interneuronal markers, including (1) V2a excitatory interneurons expressing Chx10 (5.6% ± 2.1% of all post-synaptic neurons labeled with tdTomato; Figure 4C) (Azim et al., 2014; Ni et al., 2014), (2) MSE neurons (Levine et al., 2014) labeled for Satb1 (4.4% ± 2.7%; Figure 4D) and Ap2b (7.2% ± 4.6%; Figures 4E and 4F), and (3) V1 inhibitory motor interneurons expressing FoxP2 (0.9% ± 0.9%; Figure S4A) (Bikoff et al., 2016). In contrast, spinal sensory interneuronal populations expressing Tlx3, Lbx1, or Brn3a were not *trans*-synaptically labeled with tdTomato (Figures 4G and S4B), indicating that these *inappropriate* targets are avoided by corticospinal axons regenerating into grafts. Most tdTomato-labeled neurons did not co-localize with any fate-specific neuronal markers, potentially due either to polysynaptic transmission or to HSV cytotoxicity (Lo and Anderson, 2011), which can kill infected cells.

Trans-synaptic labeling of neurons by HSV-tdTomato is typically considered an indication of the presence of active synapses (Lo and Anderson, 2011). Supporting that probability, GFP-expressing terminals of corticospinal axons regenerating into grafts were closely associated with graft tdTomato-labeled cells in bouton-like appositions (Figures 4C and 4D).

Regenerating corticospinal axons also expressed the pre-synaptic markers vGlut1 (Figures S4C and S4D) and synaptophysin (SYN; Figures S4E and S4F). Confirming the specificity of the HSV tool, no tdTomato-expressing neurons were observed in the host or graft among animals that did not receive AAV9-Cre injections. Thus, *trans*-synaptic HSV-tdTomato studies indicate that propriospinal neurons and MSE neurons are direct targets of corticospinal axons growing into grafts, receiving inputs that parallel patterns of normal spinal cord innervation by corticospinal axons (Levine et al., 2014; Ueno et al., 2018).

We also initiated *trans*-synaptic HSV-tdTomato labeling 6 months after grafting to identify long-term and persisting synaptic partners of adult corticospinal axons growing into grafts. Eight animals underwent placement of E14-derived spinal cord neural progenitor grafts into C4 bilateral dorsal column lesions (as above). Five months later, animals received cortical injections of AAV9-Cre into bilateral primary motor cortices (n = 5), as described above. One month later (6 months after grafting), animals received injections of Cre-dependent HSV-H129ΔTK-tdTomato into the primary motor cortex; that initiated HSV-tdTomato *trans*-synaptic labeling. In three other grafted subjects, Cre-dependent HSV-H129ΔTK-tdTomato was injected 6 months after grafting, without preceding injections of Cre (Lo and Anderson, 2011). All animals were perfused 3 days after HSV injection to identify a preponderance of primary synaptic partners of regenerating corticospinal axons in grafts. TdTomato-expressing *trans*-synaptically labeled graft neurons were present in all five animals that received AAV9-Cre injections (Figures 5A and 5B), but not in the three controls lacking Cre. TdTomato/GFP-expressing *trans*-synaptically labeled grafted neurons were present throughout grafts, at various rostral-to-caudal levels that were more extensively distributed than animals sacrificed 2 weeks after grafting (Figure 5A-5C). Notably, cells expressing tdTomato in 6-month grafts consisted of (1) MSE neurons labeled for Ap2b and Satbl (collectively, 25.2% of tdTomato-expressing cells; Figures 5D, 5E, 5J, and S5) (Levine et al., 2014); (2) V2a excitatory interneurons expressing Chx10 (5.5% ± 1.0% of cells; Figures 5F and 5J) (Ni et al., 2014); and (3) ChAT-expressing cholinergic neurons (motor neurons or V0c excitatory pre-motor interneurons [Zagoraiou et al., 2009]; 8.9% ± 1.6% of cells; Figures 5G, 5H, and 5J). In contrast, extremely low numbers of sensory neurons expressed HSV-tdTomato: Tlx3, 0.5% ± 0.4% (Figure 5I); Lbx1,0% (Figure S6A); and Brn3a, 1.3% ± 0.6% (Figure S6B). These patterns parallel the post-synaptic partners of corticospinal projections to the intact spinal cord (Levine et al., 2014; Ueno et al., 2018). The very low degree of sensory interneuronal innervation by *trans*-synaptic HSV-tdTomato is striking, indicating that these neurons are synaptically segregated from corticospinal inputs to grafts, even 6 months after grafting and after circuit development in grafts. Thus, regenerating adult corticospinal axons form specific synaptic contacts onto appropriate pre-motor interneuronal target neurons of grafted neural progenitor cells.

Human Neural Stem Cell Grafts to Non-human Primates

***Human Neural Stem Cell Grafts Also Adopt Diverse Spinal Cord Neuronal Fates* In Vivo—**The developmental expression of neuronal fate-specifying transcription factors is evolutionarily conserved (Lee and Pfaff, 2001). To examine the fate of human embryonic spinal cord-derived neural stem-cell grafts (566RSC-GFP cell line, gift from NeuralStem, Inc.), four rhesus monkeys underwent C7 rightsided spinal cord hemisection

lesions and received those human neural stem-cell grafts 2 weeks later with immunosuppression (see STAR Methods) (Rosenzweig et al., 2018). Three subjects were sacrificed 2-3 months later (n = 3); one additional subject received injections of biotinylated dextran amine (BDA) into bilateral motor cortices 6 weeks before sacrifice and was sacrificed 9 months after grafting (n = 1). Three months after grafting, numerous grafted cells expressed the mature neuronal marker NeuN (Figures 6A–6C). Labeling for neuronal subtype markers demonstrated the presence of several populations of interneurons in grafts, including (1) Prdm8-expressing motor interneurons (V0-2; Figure 6D); (2) V2a excitatory propriospinal interneurons expressing Chx10 (V2a; Figure 6E); (3) FoxP2-expressing inhibitory motor interneurons (V1; Figure 6F); (4) Bhlhb5-expressing interneurons (dl6, V0-2; Figure 6G) (Lai et al., 2016); (5) Brn3a-, Lbx1-, or Tlx3-expressing sensory interneurons (dl1-6; Figures 6H–6J); and (6) Pax2-expressing inhibitory interneurons (Figure 6K). As in rodent grafts, sensory interneurons labeled for Brn3a, Lbx1, or Tlx3 existed in cellular clusters (Figures 6L and 6M), and motor interneurons existed as domains that were distinct and separate among these sensory markers (Figures 6N and 6O). Distributed evenly within both of these graft domains were Pax2-expressing inhibitory interneurons (Figures 6P and 6Q), consistent with findings in rodent grafts (Figure 2). Thus, human embryonic spinal cord-derived neural stem cells exhibit the ability to differentiate into the cardinal classes of spinal interneurons. Quantification of neuronal subtypes (n = 3 animals 2-3 months after grafting; Figures 1L and 6R) demonstrated that human embryonic spinal cord-derived neural stem cells adopt a greater proportion (30.0%) of motor interneuronal fates than do rat E14 spinal cord-derived neural progenitor cells (9.7%). Human neural stem cells are cultured using EGF and FGF2, which favor motor interneuronal progenitors (Koch et al., 2009); in contrast, rodent donor neural progenitor cells were not cultured before grafting. There were no significant differences in graft fate in monkeys comparing 3- and 6-month post-graft time points.

Corticospinal Axons Preferentially Regenerate into Motor Interneuronal Domains—Corticospinal axons grow into human neural stem cell grafts (Figure 7A) (Rosenzweig et al.,2018), as observed in rodent studies. Here, we examined whether host primate corticospinal axons growing into grafts also distribute within appropriate, motor regions of the graft. Indeed, host corticospinal axons grew into grafts, demonstrated by axon penetration of NeuN-labeled regions within the lesion site (Figure 7A). Within the graft, corticospinal axons were primarily distributed in $Prdm8^+$ domains (V0-2; Figure 7B), and formed close appositions to the cell soma (Figure 7C). Corticospinal axons were either excluded or only sparsely present within $Tlx3^+$ sensory interneuronal islands in grafts (Figure 7D). These preliminary findings in the primate parallel our findings in grafts to the lesioned rat spinal cord.

DISCUSSION

Recent literature indicates that grafts of neural stem cells and neural progenitor cells to sites of spinal cord injury extend very large numbers of axons over distances up to 50 mm into the injured host spinal cord (Adler et al., 2017; Dulin et al., 2018; Kadoya et al., 2016; Lu et al., 2012, 2014) and partially improve motor performance (Curtis et al., 2018; Kadoya et al.,

2016; Kumamaru et al., 2018; Lu et al., 2012; Rosenzweig et al., 2018). However, until now, we were unaware of the phenotypic fate of the grafted rodent or human donor neural stem cells. Results of this study indicate that those grafts, isolated from developing spinal cord sources, adopt a broad, full range of early and late spinal cord neuronal markers. That likely contributes to the reconstitution of a neural environment in the lesion site that enables the regeneration of host axonal systems, including motor and sensory axons. Indeed, systems that have been refractory to efforts to promote regeneration into a lesion site, including corticospinal axons, successfully and extensively extend axons into spinal cord neural stem cell grafts (Kadoya et al., 2016; Kumamaru et al., 2018).

With what precision do host axons regenerate into grafts? Do they synapse with appropriate cellular targets replicating patterns of the developing nervous system, or is their growth random and undirected within grafts, resulting in establishment of synapses with a mixture of appropriate and inappropriate targets? In recent work, we found that host dorsal root ganglion axons regenerate to their phenotypically appropriate calretinin-expressing target neurons within distinct sensory clusters in neural progenitor cell grafts (Dulin et al., 2018). Nociceptive dorsal root ganglion axons were also reported to regenerate into appropriate adult spinal cord dorsal gray matter regions after dorsal root crush and treatment with artemin (Harvey et al., 2010). In the regenerating optic nerve, reports of reinnervation of appropriate target regions are conflicting (Benowitz et al., 2017). To date, however, there have been no reports describing the appropriateness of motor axon regeneration into neural stem cell grafts. We now find that the most important voluntary functional motor system in primates, the corticospinal projection, grows preferentially into pre-motor and motor neuronal domains in grafts and specifically avoids inappropriate spinal sensory interneuronal clusters. Using *trans*-synaptic HSV-tdTomato tracing, we further find that these regenerating axons proceed to form synapses with several normal interneuronal targets of corticospinal axons in the intact spinal cord (Ueno et al., 2018), including Chx10-expressing propriospinal neurons (Ni et al., 2014) and motor synergy encoder neurons expressing Ap2b and Satb1 (Levine et al., 2014). Thus, *adult* injured and regenerating motor axons remain capable of undergoing axonal guidance and appropriate target-finding within the developing milieu of the neural stem cell graft. These synaptic contacts are sustained over the 6-month period of grafting in rodents. Notably, these findings preliminarily extend to the primate system, wherein regenerating host corticospinal axons are present within appropriate graft motor domains and form appositional contacts with graft pre-motor interneurons. Thus, the provision of exogenous *guidance* to regenerating host axons toward appropriate neuronal targets within grafts may not be necessary, potentially simplifying the clinical translation of neural stem cell therapies for spinal cord injury.

STAR*METHODS

CONTACT FOR REAGENT AND RESOURCE SHARING

Further information and requests for resources and reagents should be directed to and will be fulfilled by the Lead Contact, Mark H. Tuszynski (mtuszynski@ucsd.edu).

EXPERIMENTAL MODEL AND SUBJECT DETAILS

Rat Studies—A total of 42 adult female Fischer 344 rats (150-250 g, Envigo, CA) were used in this study. Animals had free access to food and water throughout the study. All surgery was done under anesthesia using a combination (2 ml/kg) of ketamine (25 mg/ml), xylazine (1.3 g/ml), and acepromazine (0.25 mg/ml).

Non-human Primate Studies—We studied a total of four male rhesus macaques (*Macaca mulatta*, 7-8 year old, 8.5-11.0 kg). Subjects were housed and surgeries performed at the California National Primate Research Center (Davis, CA).

All animal subject procedures were approved by the Institutional Animal Care and Use Committees of the respective institutions. Institutional and National Institutes of Health guidelines for laboratory animal care and safety were strictly followed.

METHODS DETAILS

Spinal Cord Lesions and Rat NPC Preparation—Rat C4 dorsal column lesions were made as described previously (Kadoya et al., 2016). Briefly, after C4 laminectomy, the dorsal surface of the spinal cord was exposed. A tungsten wire knife was inserted to a depth 1 mm under the dorsal spinal cord surface; a wire arc (1.5 - 2 mm diameter) was then extruded and raised to the dorsal spinal cord surface to transect the corticospinal (CST) main tract. Complete transection of the CST was assured by exerting downward pressure on the extruded arc of the wire knife. Rat E14 spinal cord neural progenitor cells were freshly isolated from Fisher 344 rats as described previously (Kadoya et al., 2016; Lu et al., 2012). Briefly, rat E14 spinal cords were carefully dissected to avoid dorsal root ganglia (DRG) tissue contamination and dissociated with 0.125% trypsin, and dissociated cells were re-suspended at a concentration of 5.0×10^5 cells/μl in phosphate buffered saline (PBS). After trypan blue exclusion test of cell viability, 1.0×10^6 viable cells were resuspended in 2 μl PBS and injected into lesion cavities using a PicoSpritzer II (General Valve, Inc., Fairfield, NJ). Cells were grafted without additional growth factors. For phenotypic characterization experiments (Figures 1 and 2), C4-CST lesions were placed in eight rats, and E14 rat spinal cord neural progenitor cells were injected into the lesion sites on the same day. Four animals were sacrificed two-weeks post-grafting and four were sacrificed six-months post-grafting.

Corticospinal Axon Tracing—To assess corticospinal regeneration (Figure 3), AAV8 viral vectors expressing membrane-targeted tdTomato (rCOMET; 1×10^{13} genome copies/ml, Salk Viral Vector Core Facility, La Jolla, CA) was injected into 8 sites per hemisphere (coordinates from bregma (mm): A/p = +0.2 to −2.8, M/L = ± 1.7 to 3.7; D/V = 1.2) at a volume of 200 nL per site using a pulled glass micropipette (n = 4). Injection pressure and duration were controlled by a PicoSpritzer II. Two weeks after injection, C4-CST lesions were placed as described above, and GFP-negative E14 spinal cord neural progenitor cells were grafted into the lesions. Animals were sacrificed two-weeks later. For long term study of corticospinal regeneration, C4-CST lesions were placed in four rats, and GFP expressing E14 rat spinal cord neural progenitor cells were grafted into the lesion cavities on the same day. Five months later, rCOMET was injected into bilateral motor cortexes and animals were sacrificed one month later.

Anterograde *Trans*-Synaptic Mapping of Graft-Derived Neurons from Corticospinal Neurons—To assess synaptic partners of regenerating corticospinal axons (Figure 4), 200 nL AAV8-CAG-GFP (1×10^{13} genome copies/ml, AAV8-GFP) and 200 nL AAV9.CamKII0.4.Cre.SV40 (1×10^{13} genome copies/ml, AAV9-Cre) were co-injected into bilateral primary motor cortices (M1, coordinates from bregma (mm); A/P = 0.5; M/L = 3.0; D/V = 1.0, A/P= −2.0; M/L = 2.5; D/V = 1.0) two weeks before grafting (n = 4). Control animals received AAV8-GFP injections alone (n = 4). Two-weeks post-injection, all animals underwent C4-CST lesions and received GFP-negative E14 spinal cord neural progenitor cell grafts into the lesion cavity the same day. Cre-dependent HSV-H129ΔTK-tdTomato (generous gift from Dr. Lynn Enquist, CNNV, Princeton University, NJ) was injected into brain cortexes 13 days later (300 nL of the virus was injected at a single site) and animals were sacrificed three days later. After Cre-dependent HSV-H129ΔTK-tdTomato injection, rats were monitored at least twice per day for the development of symptoms (hunched back, increased activity, nasal or lacrimal excretions) to indicate HSV spread (Lo and Anderson, 2011); these were not observed until 3 days after injection. For long term HSV experiments (Figure 5), C4-CST lesions were placed in eight animals and GFP-expressing E14 spinal cord neural progenitor cells were grafted into the lesion sites. Five animals received injections of AAV9-Cre into bilateral primary motor cortex, five-months post-grafting. One month later, all animals received injections of Cre-dependent HSV-H129ΔTK-tdTomato into the motor cortices and sacrificed three days later, as described above.

Immunohistochemistry—Animals were perfused with 4% paraformaldehyde (PFA) in 0.1 M phosphate buffer (pH 7.2). Spinal cords were post-fixed and sectioned on a cryostat set at 30-μm-thick intervals in the sagittal plane. Sections were incubated with primary antibodies overnight (see Table S1) and then incubated in Alexa 488,568, or 647 conjugated donkey secondary antibodies (Invitrogen, Carlsbad, CA) and DAPI (Invitrogen). Images were captured using an Olympus AX-70 fluorescence microscope (Olympus, Tokyo, Japan) equipped with an Optronics Microire A/R digital camera Microfire A/R, (Optronics, Goleta, CA), a confocal microscope (FV-1000, Olympus, Tokyo, Japan), or the BZ-9000 digital microscope system (Keyence, Osaka, Japan).

PRIMATE PROCEDURES

Preparation of Human Spinal Cord NSCs—NSI-566RSC-GFP were provided from NeuralStem, Inc. Culture methods have been published previously (Guo et al., 2010; Rosenzweig et al., 2018). Briefly, the human embryonic cervical and upper thoracic spinal cord (gastrulation week eight) was dissociated and suspended in DMEM/F12 medium supplemented with N2 supplement, 100 mg/l human plasma apo-transferrin, 25 mg/l recombinant human insulin, 1.56 g/l glucose, 20 nM progesterone, 100 mM putrescine, and 30 nM sodium selenite. Cells were expanded in flasks coated with 100 mg/ml poly-D-lysine. 10ng/ml bFGF was added every other day. All of these cells express neural stem cell marker SOX1 and the vast majority (93.8%) of these cells express neural stem progenitor marker Nestin as previously reported (Guo et al., 2010). Cells were stored in liquid nitrogen. A day before grafting, cells were thawed, suspended at 20,000 cells/μl in a proprietary hibernation medium, and shipped overnight at 4°C.

Primate Surgery—The monkeys described here were part of a study that has been the subject of another report which states experimental methods in detail (Rosenzweig et al., 2018). Four male rhesus macaques (*Macaca mulatta*, 7-8 year old, 8.5-11.0 kg) were studied. Briefly, after deep anesthesia with 1.5%-2.5% isoflurane, the C5-6 dorsal laminae were partially removed and then right lateral hemisection lesions were created at the underlying C7 spinal cord level. Two weeks after C7 hemisection, twenty million GFP-expressing human embryonic spinal cord neural progenitor cells (NSI-566RSC-GFP, gift of NeuralStem, Inc.) were suspended in a two-part fibrin matrix containing a mixture of growth factors (Lu et al., 2012); Brain-derived neurotrophic factor (BDNF, 50 μg/mL, Peprotech, Rocky Hill, NJ), neurotrophin-3 (NT-3; 50 μg/mL, Peprotech), glial-cell-line-derived neurotrophic factor (GDNF; 10 μg/mL, Sigma, St. Louis, MO), epidermal growth factor (EGF; 10 μg/mL, Sigma), basic fibroblast growth factor (bFGF; 10 μg/mL, Sigma), acidic fibroblast growth factor (aFGF; 10 μg/mL, Sigma), hepatocyte growth factor (HGF; 10 μg/mL, Sigma), insulin-like growth factor 1 (IGF-1; 10 μg/mL, Sigma), platelet-derived growth factor (PDGFAA; 10 μg/mL, Peprotech), vascular endothelial growth factor (VEGF; 10 μg/mL, Peprotech), and a calpain inhibitor (MDL28170, 50 μM, Sigma). Cells were injected into the lesion site (n = 4). After grafting, animals received a 3-drug immunosuppressive regimen consisting of mycophenolate modafeniul (MMF; CellSept, the initial dose, 50 mg/kg twice a day), tacrolimus (FK-506; ProGraf, the initial dose, 0.5 mg/kg twice a day), and prednisone (The initial dose, 2 mg/kg/day; the maintenance dose1 mg/kg/day). Dosages of MMF and FK-506 were adjusted based on their blood concentration. Immunosuppressive therapy was continued until the time of sacrifice. Three animals were transcardially perfused with 4% PFA two to three months post-graft. For corticospinal axon tracing in one monkey, biotinylated dextran amine (BDA; 10,000 MW, 10% in water, Thermo fisher scientific, Waltham, MA) was injected into the left motor cortex over 126 sites, 300 nL/site, seven months post-grafting. Animals were transcardially perfused with 4% PFA six weeks later. C6-8 segments were horizontally sectioned on a sliding microtome set at 30 μm-thick intervals.

QUANTIFICATION AND STATISTICAL ANALYSIS

Quantification of Neuronal Subtypes in Rat Spinal Cord NPC Grafts—To quantify neuronal subtypes in E14 rat neural progenitor cell grafts (two weeks post-grafting), neuronal subtype transcription factor (Brn3a, Tlx3, Lbx1, Pax2, Bhlhb5, Prdm8, Chx10, Lhx3, Foxp1, FoxP2, or Isl1/2) and NeuN co-labeled sections were used (n = 4 animals, two sections, two fields per animal per label). Images were taken from two fields at the graft epicenter in each subject on a confocal microscope (200X magnification, Olympus FV-1000). The number of neuronal subtype transcription factor- or NeuN-expressing cells was counted for each label on ImageJ. The ratio of subtype marker-expressing cells to total number of NeuN cells was calculated and then averaged among groups. To determine the proportion of sensory interneuronal derivatives, Tlx3, Lbx1, Brn3a, and NeuN labeled sections were used (4 animals, 2 sections, 2 fields per section, per animal). Sensory interneuronal markers (Tlx3, Lbx1, and Brn3a) were labeled with Alexa 568 and NeuN was labeled with Alexa 647 since there are Tlx3, Lbx1, and Brn3a colabeled neurons within the graft. Images were taken from two randomly selected fields in graft on a confocal microscope (x200 magnification, Olympus FV-1000). Quantification was performed as

described above. To quantify mature neuronal subtypes in the graft (six-month post-grafting), neuronal subtype marker (calmodulin-dependent protein kinase II (CAMKII), choline acetyltransferase (ChAT), or GABA) and NeuN co-labeled sections were used (n = 5 animals, 2 sections, 2-6 fields per animal per label). Images were taken from randomly selected two to six fields in each subject by using a confocal microscopy (x400 magnification).The number of subtype marker or NeuN expressing cells were manually counted and then the number of neuronal subtype marker expressing cells were divided by the number of NeuN expressing cells and then averaged among groups. To quantify cell type-specific markers within Tlx3-expressing graft regions, Brn3a, Chx10, FoxP2, and Isl1/2 + cells were counted within the Tlx3 + interneuronal clusters, and outside of the Tlx3 + interneuronal clusters (n = 4 animals, 2 sections, 2 fields per animal per label). Tlx3 + clusters were outlined by connecting Tlx3 + cells on the edge of Tlx3 + neuronal clusters. Proportion of motor neuronal derivatives was calculated by adding mean values of Prdm8, Chx10, and FoxP2 expressing cells.

Quantification of Corticospinal Regeneration Domain Regions—Quantification of host axon regeneration was performed using images taken on the confocal microscope (200X magnification, n = 4 animals, 2 sections per animal, 2 fields per section). Every 6^{th} section was labeled for GFP, RFP, and Tlx3, and the two most medial sections containing the corticospinal main tract in the dorsal column region were chosen for quantification. The outer margins of Tlx3 + cell clusters were outlined, and the pixel intensity of regenerating corticospinal axons within grafts was thresholded and measured in ImageJ.

Quantification of HSV-Labeled Cells in grafts—Quantification of HSV-labeled sensory and pre-motor interneurons was performed using RFP and Ap2b, Satb1, Chx10, ChAT, FoxP2, Brn3a, Tlx3, or Lbx1, co-labeled sections (n = 4 or 5 animals, 2-5 sections per graft). Images were taken from all fields containing tdTomato labeled cells in each subject on a confocal microscope (200× magnification, Olympus FV-1000) and then tdTomato, AP2b, Satb1, Chx10, ChAT, FoxP2, Brn3a, Tlx3, or Lbx1, labeled cells and double labeled cells were manually counted (Cell diameter > 5 um). Results were expressed as the proportion of interneuronal marker-expressing cells (Ap2b, Satb1, Chx10, ChAT, FoxP2, Brn3a, Tlx3, or Lbx1) divided by the number of tdTomato-labeled cells, and then averaged among groups.

Quantification of Neuronal Subtypes in Human Spinal Cord NSC Grafts—To quantify neuronal subtypes in human spinal cord neural stem cell grafts, neuronal subtype transcription factor (Brn3a, Tlx3, Lbx1, Pax2, Bhlhb5, Prdm8, Chx10, or FoxP2) and NeuN co-labeled sections were used (n = 3 animals at 2 to 3 months post-grafting, one section quantified per subject). Transcription factor- or NeuN-expressing cells were counted in 2-4 randomly selected fields (x200 magnification, Olympus FV-1000). Quantification was performed as described above.

Supplementary Material

Refer to Web version on PubMed Central for supplementary material.

ACKNOWLEDGMENTS

We thank L. Graham, E. Staufenberg, J. Conner, and J. Weberfor technical assistance; T. Müller and C. Birchmeier, Max-Delbrück-Center for Molecular Medicine, Berlin, Germany, for providing Tlx3 and Lbx1 antibodies; S. Ross, University of Pittsburgh, Pittsburgh, for providing Bhlhlb5 and Prdm8 antibodies; and Lynn Enquist, CNNV, Princeton University, NJ, for providing Cre-dependent HSV-H129ΔTK-tdTomato. Human 566RSC-UBQT neural stem cells were a gift from NeuralStem, Inc. Supported by the Veterans Administration Gordon Mansfield Spinal Cord Injury Consortium (to M.H.T.), the NIH (NS042291 and EB014986, to M.H.T.); the Craig H. Neilsen Foundation (to H.K. and K.K.); the Japan Society for the Promotion of Science (to H.K. and K.K.); the Bernard and Anne Spitzer Charitable Trust (to M.H.T.); and the Dr. Miriam and Sheldon G. Adelson Medical Research Foundation (to M.H.T.).

REFERENCES

Adler AF, Lee-Kubli C, Kumamaru H, Kadoya K, and Tuszynski MH (2017). Comprehensive monosynaptic rabies virus mapping of host connectivity with neural progenitor grafts after spinal cord Injury. Stem Cell Reports 8, 1525–1533. [PubMed: 28479302]

Alaynick WA, Jessell TM, and Pfaff SL (2011). SnapShot: spinal cord development. Cell 746, 178-178-e171.

Alvarez FJ, Jonas PC, Sapir T, Hartley R, Berrocal MC, Geiman EJ, Todd AJ, and Goulding M (2005). Postnatal phenotype and localization of spinal cord V1 derived interneurons. J. Comp. Neurol 493, 177–192. [PubMed: 16255029]

Arber S (2012). Motor circuits in action: specification, connectivity, and function. Neuron 74, 975–989. [PubMed: 22726829]

Azim E, Jiang J, Alstermark B, and Jessell TM (2014). Skilled reaching relies on a V2a propriospinal internal copy circuit. Nature 508, 357–363. [PubMed: 24487617]

Benowitz LI, He ZG, and Goldberg JL (2017). Reaching the brain: Advances in optic nerve regeneration. Exp. Neurol 287, 365–373. [PubMed: 26746987]

Bikoff JB, Gabitto MI, Rivard AF, Drobac E, Machado TA, Miri A, Brenner-Morton S, Famojure E, Diaz C, Alvarez FJ, et al. (2016). Spinal inhibitory interneuron diversity delineates variant motor microcircuits. Cell 165, 207–219. [PubMed: 26949184]

Cheng L, Arata A, Mizuguchi R, Qian Y, Karunaratne A, Gray PA, Arata S, Shirasawa S, Bouchard M, Luo P, et al. (2004). Tlx3 and Tlx1 are postmitotic selector genes determining glutamatergic over GABAergic cell fates. Nat. Neurosci 7, 510–517. [PubMed: 15064766]

Curtis E, Martin JR, Gabel B, Sidhu N, Rzesiewicz TK, Mandeville R, Van Gorp S, Leerink M, Tadokoro T, Marsala S, et al. (2018). A first-inhuman, phase i study of neural stem cell transplantation for chronic spinal cord injury. Cell Stem Cell 22, 941–950.e6. [PubMed: 29859175]

Del Barrio MG, Bourane S, Grossmann K, Schiile R, Britsch S, O'Leary DD, and Goulding M (2013). Atranscription factorcode defines nine sensory interneuron subtypes in the mechanosensory area of the spinal cord. PLoS ONE 8, e77928. [PubMed: 24223744]

Dougherty KJ, and Kiehn O (2010). Firing and cellular properties ofV2a interneurons in the rodent spinal cord. J. Neurosci 30, 24–37. [PubMed: 20053884]

Dulin JN, Adler AF, Kumamaru H, Poplawski GHD, Lee-Kubli C, Strobl H, Gibbs D, Kadoya K, Fawcett JW, Lu P, and Tuszynski MH (2018). Injured adult motor and sensory axons regenerate into appropriate organotypic domains of neural progenitor grafts. Nat. Commun 9, 84. [PubMed: 29311559]

Francius C, Harris A, Rucchin V, Hendricks TJ, Stam FJ, Barber M, Kurek D, Grosveld FG, Pierani A, Goulding M, and Clotman F (2013). Identification of multiple subsets ofventral interneurons and differential distribution along the rostrocaudal axis ofthe developing spinal cord. PLoS ONE 8, e70325. [PubMed: 23967072]

Goulding M (2009). Circuits controlling vertebrate locomotion: moving in a new direction. Nat. Rev. Neurosci 10, 507–518. [PubMed: 19543221]

Gross MK, Dottori M, and Goulding M (2002). Lbx1 specifies somatosensory association interneurons in the dorsal spinal cord. Neuron 34, 535–549. [PubMed: 12062038]

Guo X, Johe K, Molnar P, Davis H, and Hickman J (2010). Characterization of a human fetal spinal cord stem cell line, NSI-566RSC, and its induction to functional motoneurons. J. Tissue Eng. Regen. Med 4, 181–193. [PubMed: 19950213]

Harvey P, Gong BJ, Rossomando AJ, and Frank E (2010). Topographically specific regeneration of sensory axons in the spinal cord. Proc. Natl. Acad. Sci. USA 107, 11585–11590. [PubMed: 20534446]

Hilton BJ, and Bradke F (2017). Can injured adult CNS axons regenerate by recapitulating development? Development 144, 3417–3429. [PubMed: 28974639]

Kadoya K, Lu P, Nguyen K, Lee-Kubli C, Kumamaru H, Yao L, Knackert J, Poplawski G, Dulin JN, Strobl H, et al. (2016). Spinal cord reconstitution with homologous neural grafts enables robust corticospinal regeneration. Nat. Med 22, 479–487. [PubMed: 27019328]

Kiehn O (2016). Decoding the organization ofspinal circuitsthat control locomotion. Nat. Rev. Neurosci 17, 224–238. [PubMed: 26935168]

Koch P, Opitz T, Steinbeck JA, Ladewig J, and Br€stle O (2009). A rosette-type, self-renewing human ES cell-derived neural stem cell with potential for in vitro instruction and synaptic integration. Proc. Natl. Acad. Sci. USA 106, 3225–3230. [PubMed: 19218428]

Kumamaru H, Kadoya K, Adler AF, Takashima Y, Graham L, Coppola G, and Tuszynski MH (2018). Generation and post-injury integration of human spinal cord neural stem cells. Nat. Methods 15, 723–731. [PubMed: 30082899]

Lai HC, Seal RP, and Johnson JE (2016). Making sense out ofspinal cord somatosensory development. Development 143, 3434–3448. [PubMed: 27702783]

Lee SK, and Pfaff SL (2001). Transcriptional networks regulating neuronal identity in the developing spinal cord. Nat. Neurosci 4 (Suppl), 1183–1191. [PubMed: 11687828]

Levine AJ, Hinckley CA, Hilde KL, Driscoll SP, Poon TH, Montgomery JM, and Pfaff SL (2014). Identification of a cellular node for motor control pathways. Nat. Neurosci 17, 586–593. [PubMed: 24609464]

Lo L, and Anderson DJ (2011). A Cre-dependent, anterograde transsynaptic viral tracer for mapping output pathways of genetically marked neurons. Neuron 72, 938–950. [PubMed: 22196330]

Lu P, Wang Y, Graham L, McHale K, Gao M, Wu D, Brock J, Blesch A, Rosenzweig ES, Havton LA, et al. (2012). Long-distance growth and connectivity of neural stem cells after severe spinal cord injury. Cell 150, 1264–1273. [PubMed: 22980985]

Lu P, Woodruff G, Wang Y, Graham L, Hunt M, Wu D, Boehle E, Ahmad R, Poplawski G, Brock J, et al. (2014). Long-distance axonal growth from human induced pluripotent stem cells after spinal cord injury. Neuron 83, 789–796. [PubMed: 25123310]

Lu DC, Niu T, and Alaynick WA (2015). Molecular and cellular development of spinal cord locomotor circuitry. Front. Mol. Neurosci 8, 25. [PubMed: 26136656]

Lu P, Ceto S, Wang Y, Graham L, Wu D, Kumamaru H, Staufenberg E, and Tuszynski MH (2017). Prolonged human neural stem cell maturation supports recovery in injured rodent CNS. J. Clin. Invest 127, 3287–3299. [PubMed: 28825600]

Medalha CC, Jin Y, Yamagami T, Haas C, and Fischer I (2014). Transplanting neural progenitors into a complete transection model of spinal cord injury. J. Neurosci. Res 92, 607–618. [PubMed: 24452691]

Mizuguchi R, Kriks S, Cordes R, Gossler A, Ma Q, and Goulding M (2006). Ascl1 and Gsh1/2 control inhibitory and excitatory cell fate in spinal sensory interneurons. Nat. Neurosci 9, 770–778. [PubMed: 16715081]

Müller T, Brohmann H, Pierani A, Heppenstall PA, Lewin GR, Jessell TM, and Birchmeier C (2002). The homeodomain factor lbx1 distinguishes two major programs of neuronal differentiation in the dorsal spinal cord. Neuron 34, 551–562. [PubMed: 12062039]

Ni Y, Nawabi H, Liu X, Yang L, Miyamichi K, Tedeschi A, Xu B, Wall NR, Callaway EM, and He Z (2014). Characterization of long descending premotor propriospinal neurons in the spinal cord. J. Neurosci 34, 9404–9417. [PubMed: 25009272]

O'Shea TM, Burda JE, and Sofroniew MV (2017). Cell biology ofspinal cord injury and repair. J. Clin. Invest 127, 3259–3270. [PubMed: 28737515]

Rosenzweig ES, Brock JH, Lu P, Kumamaru H, Salegio EA, Kadoya K, Weber JL, Liang JJ, Moseanko R, Hawbecker S, et al. (2018). Restorative effects of human neural stem cell grafts on the primate spinal cord. Nat. Med 24, 484–90. [PubMed: 29480894]

Sathyamurthy A, Johnson KR, Matson KJE, Dobrott CI, Li L, Ryba AR, Bergman TB, Kelly MC, Kelley MW, and Levine AJ (2018). Massively parallel single nucleus transcriptional profiling defines spinal cord neurons and their activity during behavior. Cell Rep. 22, 2216–2225. [PubMed: 29466745]

Ueno M, Nakamura Y, Li J, Gu Z, Niehaus J, Maezawa M, Crone SA, Goulding M, Baccei ML, and Yoshida Y (2018). Corticospinal circuits from the sensory and motor cortices differentially regulate skilled movements through distinct spinal interneurons. Cell Rep. 23, 1286–1300e7. [PubMed: 29719245]

Wojaczynski GJ, Engel EA, Steren KE, Enquist LW, and Patrick Card J (2015). The neuroinvasive profiles of H129 (herpes simplex virus type 1) recombinants with putative anterograde-only transneuronal spread properties. Brain Struct. Funct 220, 1395–1420. [PubMed: 24585022]

Xu Y, Lopes C, Qian Y, Liu Y, Cheng L, Goulding M, Turner EE, Lima D, and Ma Q (2008). Tlx1 and Tlx3 coordinate specification of dorsal horn pain-modulatory peptidergic neurons. J. Neurosci 28, 4037–4046. [PubMed: 18400903]

Yan J, Xu L, Welsh AM, Hatfield G, Hazel T, Johe K, and Koliatsos VE (2007). Extensive neuronal differentiation of human neural stem cell grafts in adult rat spinal cord. PLoS Med. 4, e39. [PubMed: 17298165]

Zagoraiou L, Akay T, Martin JF, Brownstone RM, Jessell TM, and Miles GB (2009). A cluster of cholinergic premotor interneurons modulates mouse locomotor activity. Neuron 64, 645–662. [PubMed: 20005822]

Highlights

- Spinal neuroprogenitor grafts spontaneously segregate into motor or sensory domains
- Grafted neuroprogenitor cells adopt diverse fates resembling the normal spinal cord
- Corticospinal axons specifically regenerate into motor domains of grafts
- Regenerating corticospinal axons avoid inappropriate sensory targets in grafts

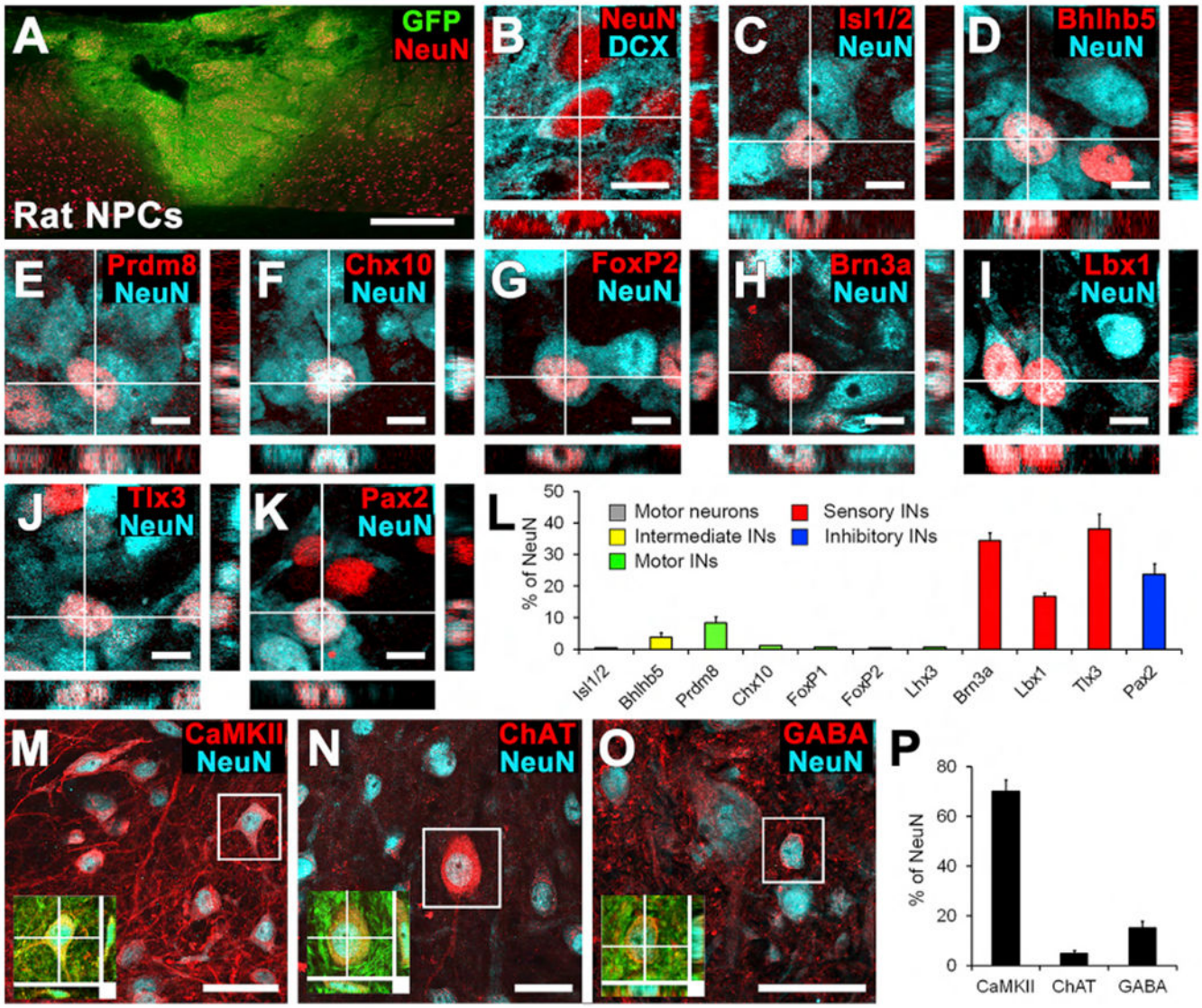

Figure 1. Phenotypic Characterization of Rat Spinal Cord Neural Progenitor Cell Grafts at 2 Weeks and at 6 Months after Grafting

(A) GFP-expressing rat spinal-cord multipotent neural progenitor cell graft transplanted 2 weeks earlier into C4 bilateral dorsal spinal cord lesion cavity. Sagittal section; rostral is left, and caudal is right. Red, NeuN. Scale bar, 500 μm.

(B) Confocal thin-plane image of the neuronal markers NeuN and doublecortin (DCX), 2 weeks after grafting. This immature graft expressed the early neuronal marker DCX. Scale bar, 10 μm.

(C–L) NeuN-expressing neurons in grafts express (C) the motor neuronal marker Isl1/2; (D) the intermediate-ventral interneuronal marker Bhlhb5 (dl6 and V1–2); (E) the intermediate-ventral interneuronal marker Prdm8 (V0–2); (F) the V2a excitatory interneuronal marker Chx10; (G) the V1 inhibitory interneuronal maker FoxP2; (H) the sensory interneuronal marker Brn3a (dl1–3); (I) the sensory interneuronal marker Lbx1 (dl4–6); (J) the sensory

interneuronal markerTlx3 (dl3, dlL_B, and dl5); and (K) the inhibitory interneuronal marker Pax2. Scale bars, 10 μm.

(L) Quantification of graft-derived neuronal subtypes demonstratesthat most grafted neurons express sensory interneuronal markers 2 weeks after grafting. INs, interneurons. n = 4 animals.

(M–O) Thin-plane confocal images of spinal cord neural progenitor cell grafts 6 months after transplantation. NeuN-expressing neurons in grafts express (M) CaMKII, (N) ChAT, or (O) GABA. Scale bars, 40 μm. Insets show co-localization of GFP, NeuN, and (M) CaMKII, (N) ChAT, or (O) GABA.

(P) Quantification of neuronal subtypes: after 6 months, most neural progenitor cell-derived neurons express CaMKII, which is expressed in excitatory neurons. Means ± SEM.

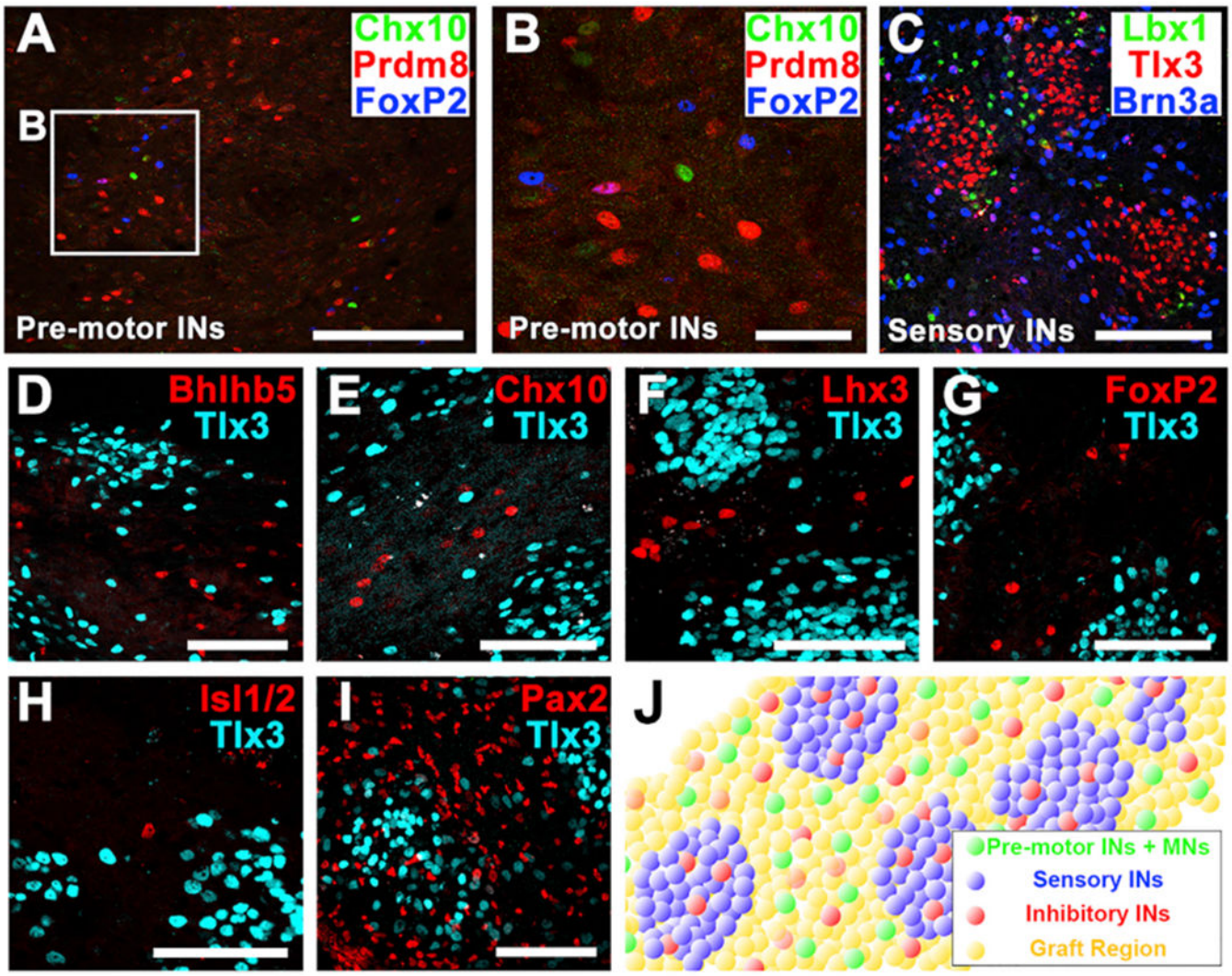

Figure 2. The Spatial Distribution of Neuronal Subtypes in 2-Week-Old Grafts

(A and B) Immunolabeling for three motor interneuronal markers (Chx10, Prdm8, and FoxP2) demonstrating motor interneurons (INs) exist sparsely within the graft. Boxed area is shown in (B). Scale bars, 200 μm (A) and 50 μm (B).

(C) Immunolabeling for three sensory interneuronal markers (Tlx3, Lbx1, and Brn3a) demonstrating clustering into similar regional clusters. Scale bar, 100 μm.

(D–I) Immunolabeling for the sensory interneuronal marker Tlx3 with the pre-motor interneuronal markers (D) Bhlhb5, (E) Chx10, (F) Lhx3, (G) FoxP2, (H)the motor neuronal marker Isl1/2, and (I) the pan-inhibitory interneuronal marker Pax2. Note that grafted neurons expressing pre-motor interneuronal markers are distributed in between, but not within, sensory interneuronal clusters. Pax2-expressing inhibitory interneurons are uniformly dispersed throughout the graft in both motor and sensory domains. Scale bars, 100 μm.

(J) Schematic representation of distribution of pre-motor interneurons and motorneurons (pre-motor INs + MNs, green), sensory interneurons (sensory INs, blue), and inhibitory interneurons (red) within spinal cord neural progenitor cell graft (yellow).

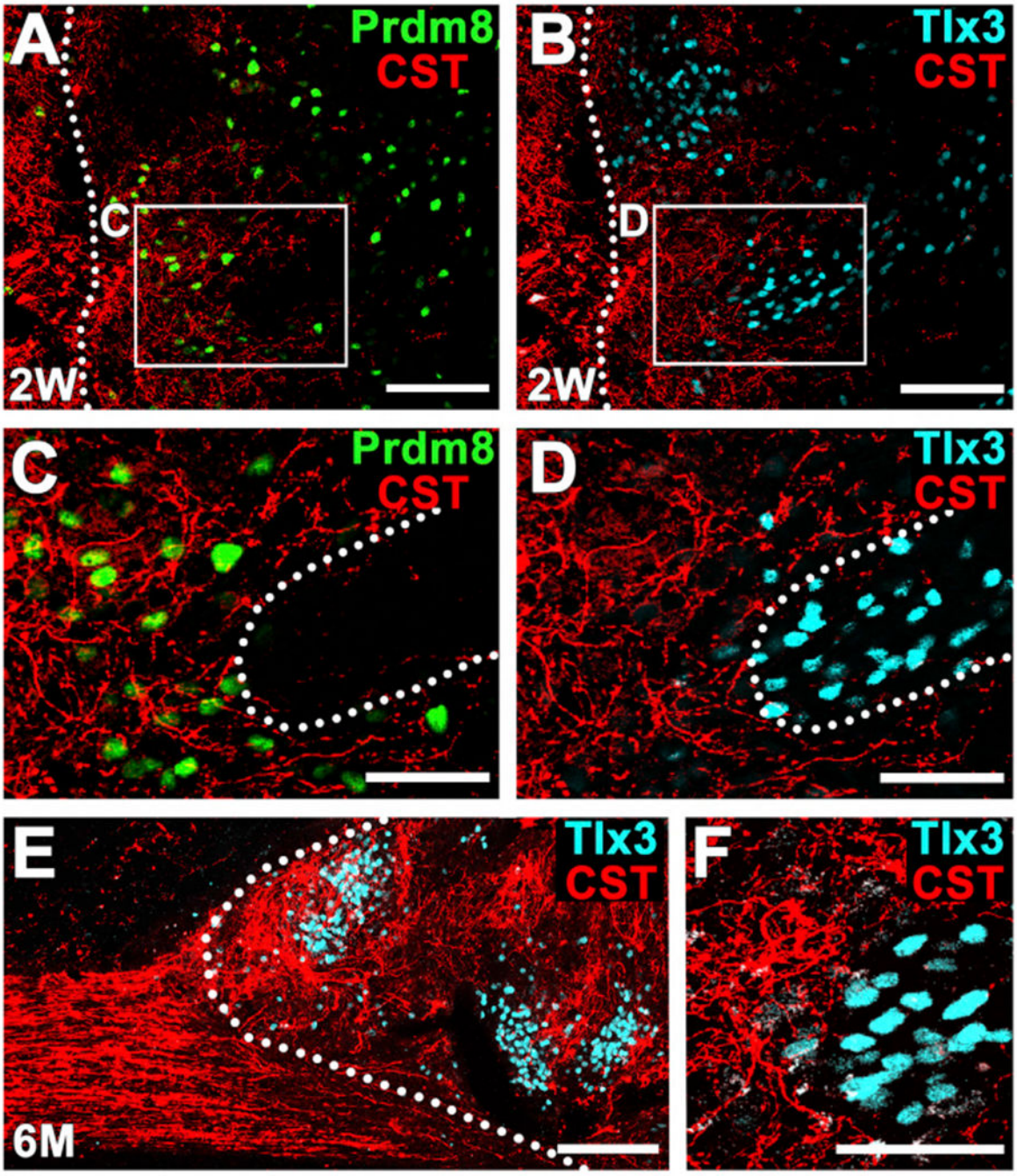

Figure 3. Host Corticospinal Axon Regeneration into Rat Neural Progenitor Cell Graft

(A–D) Corticospinal axons (red) are present within regions of Prdm8-expressing V1-2 pre-motor interneurons (A and C) (green) and are attenuated in clusters of Tlx3-expressing sensory interneurons (B and D) (cyan) within the graft 2 weeks after grafting. Dotted lines indicate rostral host-graft border (A and B) and motor-sensory domain border (C and D). Sagittal section; rostral is left. Thin-plane confocal images of boxed areas are shown in (C) and (D). Scale bars, 100 μm (A and B) and 50 um (C and D).

(E and F) Six months after grafting, corticospinal axon density remains greater in grafts regions free of Tlx3-expressing sensory interneuronal clusters. Dotted line indicates host-graft border. Left, rostral; right, caudal. Scale bars, 200 μm (E) and 50 μm (F).

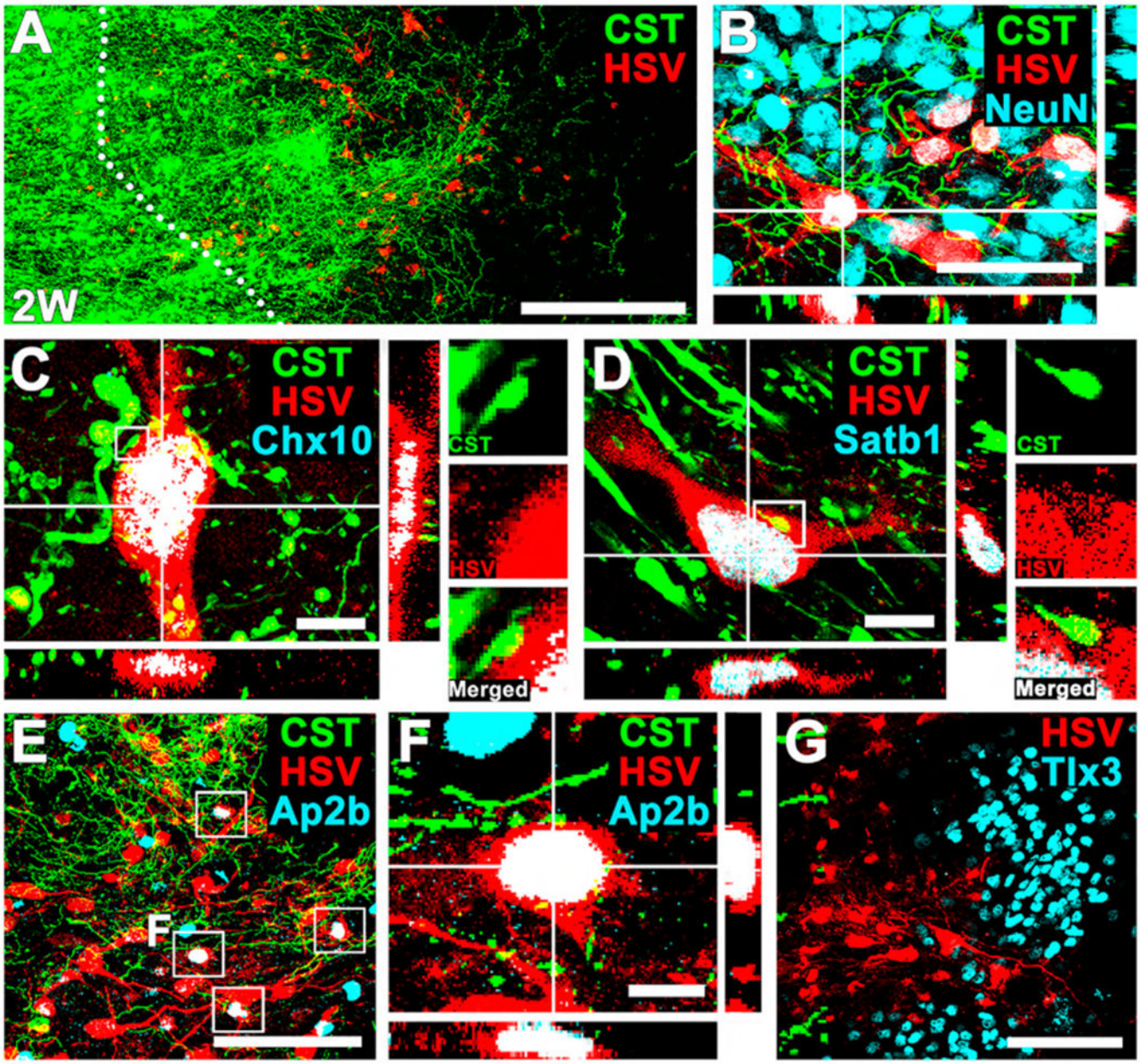

Figure 4. Synaptic Partners of Regenerating Corticospinal Axons in Rat Neural Progenitor Cell Grafts: HSV *Trans*-synaptic Labeling

(A) Double labeling for corticospinal axons regenerating into grafts (GFP) and tdTomato (HSV), 2 weeks after grafting. Dotted lines indicate rostral host-graft border. Sagittal section; rostral is left. Scale bar, 100 μm.

(B) Immunolabeling for GFP (corticospinal axons), tdTomato (HSV), and NeuN, 2 weeks after grafting, showing *trans*-synaptically labeled cells in grafts that express NeuN in regions of corticospinal axons. Scale bar, 50 μm.

(C and D) Cells *trans*-synaptically labeled for tdTomato express (C) Chx10 and (D) Satb1. Side panels demonstrate that bouton-like corticospinal appositions are present on the surface of *trans*-synaptically labeled cells in graft. Scale bars, 10 μm.

(E and F) Cell *trans*-synaptically labeled for tdTomato also express the motor synergy encoder (MSE) neuronal marker Ap2b within regions of corticospinal regeneration. Boxed area indicates tdTomato (HSV) and Ap2b double-labeled cells in grafts. (F) shows boxed area in (E). Scale bars, 100 μm (E) and 10 μm (F).

(G) However, cells *trans*-synaptically labeled with tdTomato do not express the sensory interneuronal marker Tlx3. Left, rostral; right, caudal. Scale bar, 100 μm.

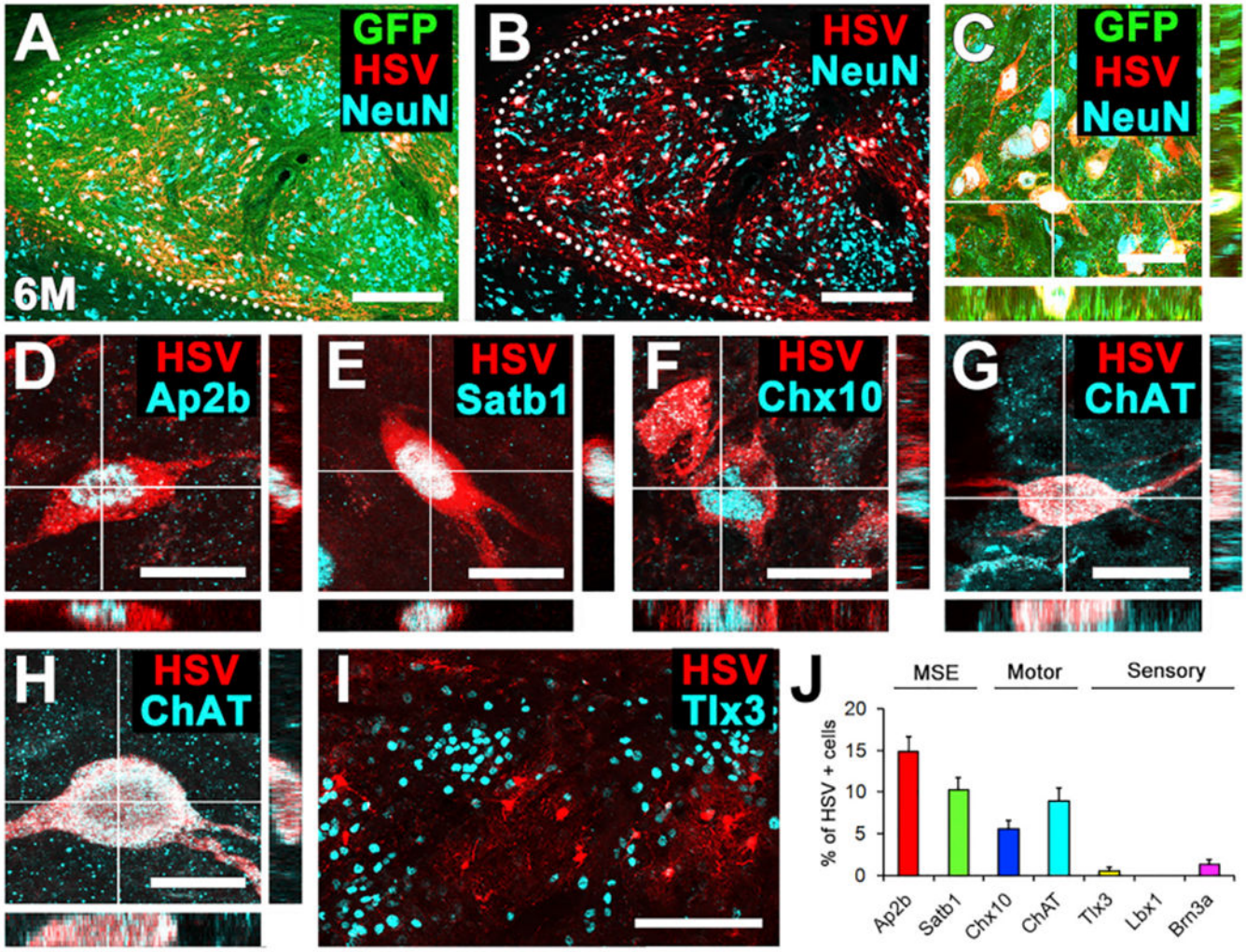

Figure 5. Anterograde Corticospinal HSV Tracing after 6 Months: Specificity of Graft Innervation from Host

(A–C) Cells in grafts *trans*-synaptically labeled with tdTomato (red, HSV) are readily evident with the GFP-expressing graft, 6 months after implantation into spinal cord lesion cavity. Sagittal section; rostral left, caudal right. Dotted line indicates rostral host-graft border. Scale bars, 250 μm (A and B) and 50 μm (C).

(D–I) Characterization of graft neurons *trans*-synaptically labeled with tdTomato after motor cortex injections of HSV. Synaptically connected tdTomato^{+} graft-derived neurons include (D) Ap2b or (E) Satb1^{+} MSE neurons, (F) Chx10+ V2a, and (G and H) cholinergic neurons. Cholinergic neurons are likely to be both (G) V0c interneurons and (H) alpha motor neurons based upon their size and morphology. Scale bars, 20 μm.

(I) *Trans*-synaptically labeled tdTomato-expressing neurons located in domains outside *inappropriate* sensory interneuronal clusters (Tlx3^{+}). Left, rostral; right, caudal. Scale bar, 200 μm.

(J) Quantification of HSV-tdTomato *trans*-synaptically labeled neurons (n = 4 animals). Means ± SEM.

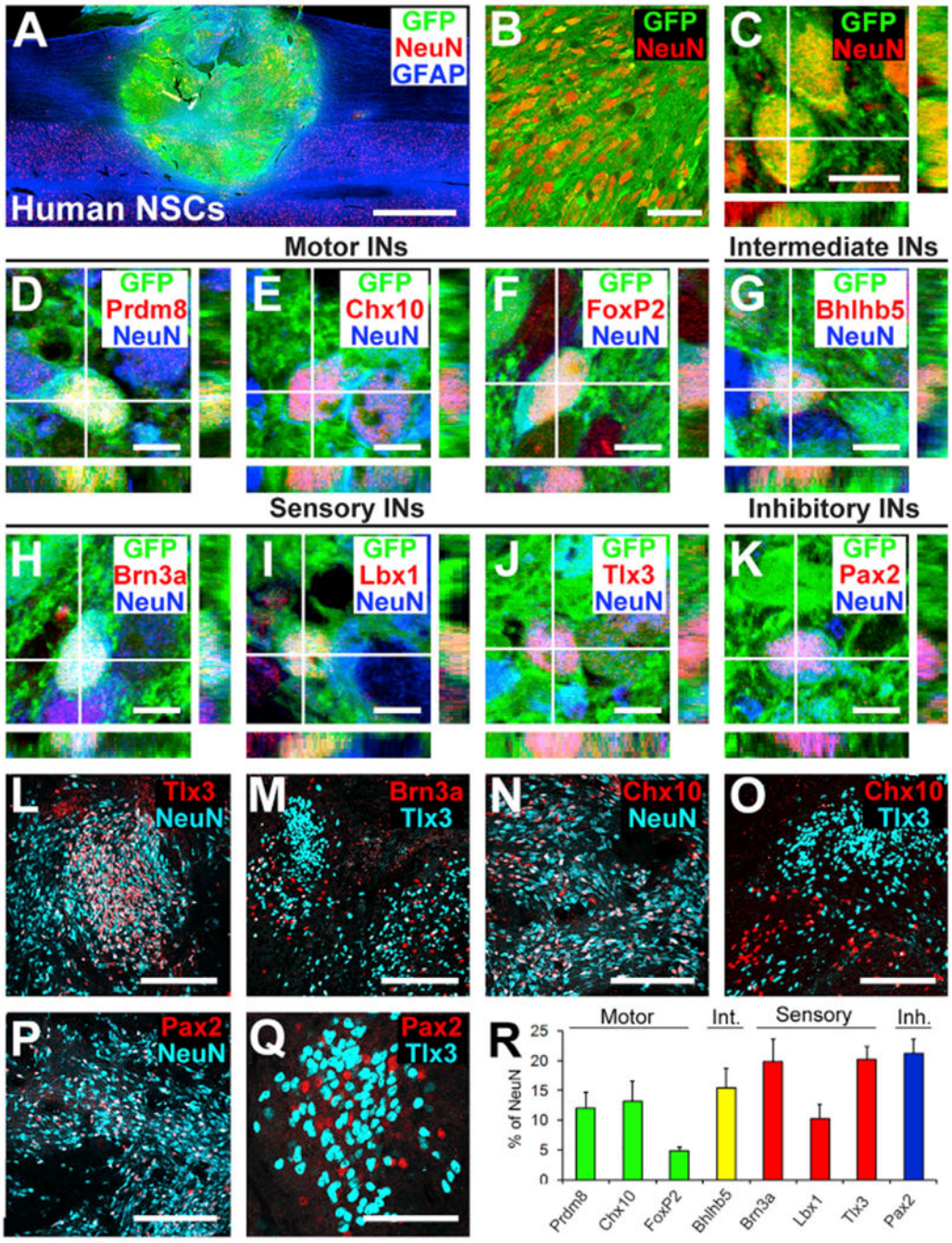

Figure 6. Phenotypic and Spatial Characterization of Human Spinal Cord Neural Stem Cell Grafts into Primates

(A) Sagittal overview of human spinal cord-derived neural stem cell (NSC) graft placed in C7 right lateral hemisection lesion cavity in an adult rhesus monkey, 3 month time point. Horizontal section, rostral is left. Graft expresses GFP; section is also labeled for NeuN and GFAP. Graft survives and fills the lesion cavity. Left, rostral; right, caudal. Scale bar, 2 mm. (B and C) Confocal images of GFP and the neuronal marker NeuN, demonstrating human graft (GFP) differentiation into NeuN-expressing neurons, 3 months after grafting. Scale bars, 10 μm (C) and 50 μm (D).

(D–K) Confocal images of sections labeled for GFP, NeuN, and various interneuronal markers. GFP/NeuN-expressing neurons express the pre-motor interneuronal markers (D) Prdm8 for V0 interneurons, (E) Chx10 for V2a excitatory pre-motor interneurons, (F) FoxP2 for VI inhibitory interneurons, (G) Bhlhb5 for intermediate interneurons (dl6 and V1–2), (H) Brn3a for sensory interneurons (dl1–3), (I) Lbx1 for sensory interneurons (dl4–6), (J) Tlx3 for sensory interneurons (dl3, dlL_B, and dl5), and (K) Pax2 for inhibitory interneurons. Scale bars, 10 μm. (L and M) Tlx3- (L) and Brn3a- (M) expressing sensory interneurons are present in clusters in human NSC grafts, similar to observations in rodent models. Scale bars, 200 μm.

(N and O) Chx10-expressing V2a interneurons are present within human NSC grafts (N) and are distributed apart from regions of Tlx3-expressing sensory interneuronal clusters (O). Scale bars, 200 μm.

(P and Q) Pax2-expressing inhibitory interneurons are distributed uniformly in grafts (P) and are also present within sensory interneuronal clusters (Q). Scale bars, 200 μm (P) and 50 μm (Q).

(R) Quantification of neuronal subtypes within human NSC grafts in monkeys (n = 3). Human NSC grafts contain higher proportions of pre-motor interneuronal markers than rat neural stem cell grafts (compare to Figure 1L). Int., intermediate; Inh., inhibitory. Means ± SEM.

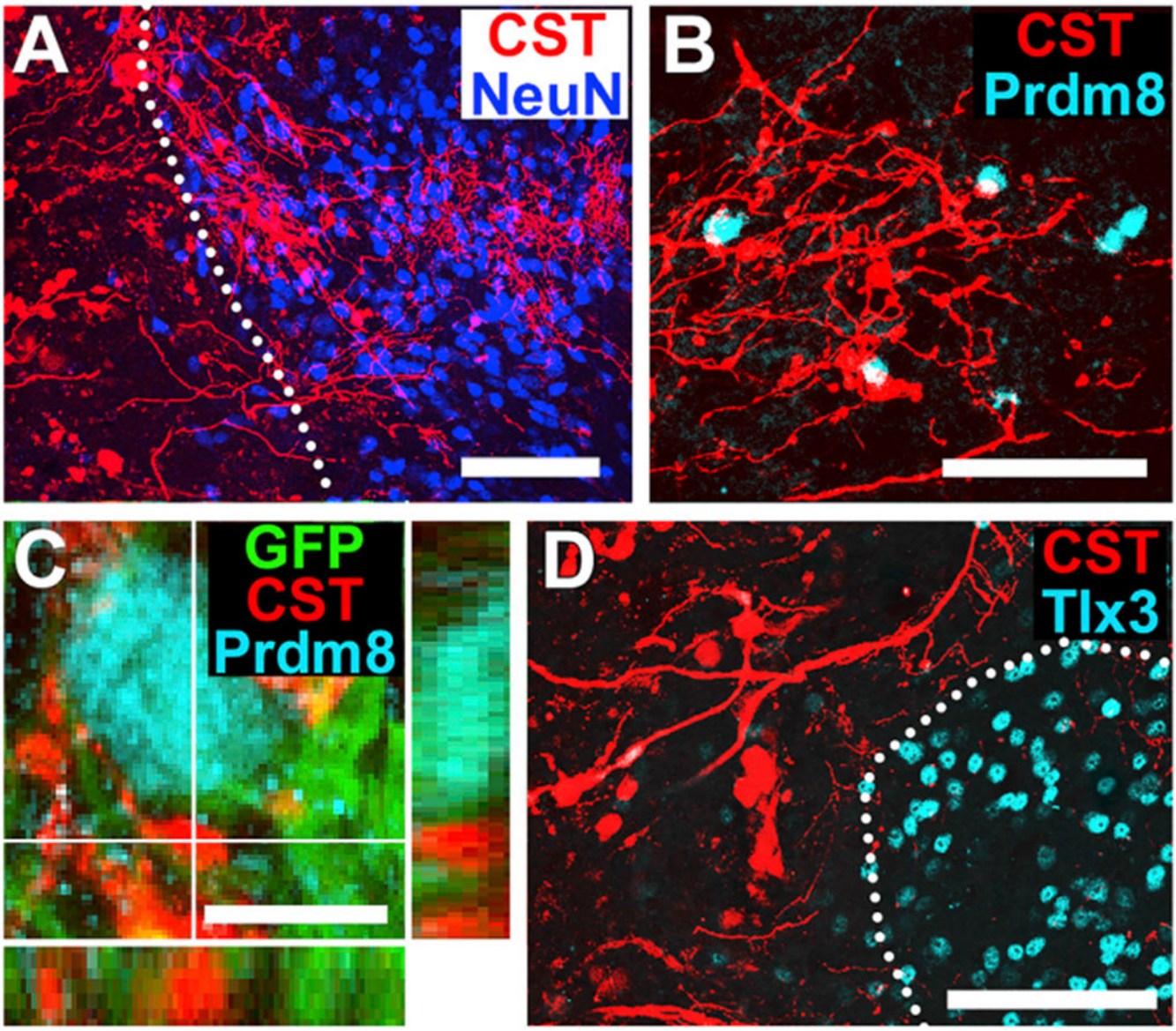

Figure 7. Primate Corticospinal Axons Regenerating into Human Neural Stem Cell Grafts Avoid Sensory Interneuronal Clusters

(A) Corticospinal axons (CST) labeled for BDA are present within neural stem graft labeled for NeuN. Nine months after grafting. Horizontal section; dotted lines indicate rostral host-graft border. Scale bar, 50 μm.

(B) BDA-labeled corticospinal axons (CST) regenerate among Prdm8-expressing (V0–2) pre-motor interneurons in grafts. Scale bar, 50 μm.

(C) Corticospinal axons (CST, red) form close appositions with the surface of Prdm8-expressing (cyan) graft neurons. Scale bar, 10 um.

(D) BDA-labeled corticospinal axon (CST) density is generally attenuated in regions of Tlx-3 sensory interneuronal clusters. Dotted lines indicate sensory interneuronal domains. Left, rostral; right, caudal. Scale bars, 100 μm.

KEY RESOURCES TABLE

REAGENT or RESOURCE	SOURCE	IDENTIFIER
Antibodies		
Mouse Brn3a	Millipore	Cat# MAB1585
Rabbit CaMKII	Genetex	Cat# GTX61641
Goat ChAT	Millipore	Cat# Ab144P
Sheep Chx10	Abcam	Cat# ab16141
Goat Doublecortin (DCX)	Santa Biotechnology	Cat# sc-8066
Rabbit FoxP1	Abcam	Cat# ab16445
Rabbit FoxP2	Abcam	Cat# ab16046
Rabbit GABA	Sigma	Cat# A2052
Mouse Islet 1/2	DSHB	Cat# 39.4D5-c
Rabbit Lhx3	Genetex	Cat# GTX14555
Mouse NeuN	Millipore	Cat# MAB377
Rabbit NeuN	Biosensis	Cat# R-3770-100
Mouse Nkx2.2	DSHB	Cat# 74.5A5-c
Mouse Nkx6.1	DSHB	Cat# F55A12-c
Rabbit Olig2	IBL	Cat# 18953
Rabbit Pax2	Life Technology	Cat# 716000
Mouse Pax7	DSHB	Cat# Pax7-c
Rabbit RFP	Abcam	Cat# ab34771
Gout mCherry	Sicgen	Cat# AB0040
Mouse Satb1	Santa Biotechnology	Cat# sc-376096
Goat Satb1	Santa Biotechnology	Cat# sc-5989
Rabbit Sox2	Abcam	Cat# ab97959
Goat Sox2	Santa Biotechnology	Cat# sc-17320
Mouse Synaptophysin (SYN)	Novus bio	Cat# NBP1-19222
Rabbit Tcfap2b (Ap2b)	Santa Biotechnology	Cat# sc-8976
Rabbit vGlut1	Sigma	Cat# V0389-200
Bacterial and Virus Strains		
AAV8 viral vectors expressing membrane-targeted tdTomato (rCOMET)	Salk Viral Vector Core Facility	N/A
AAV8-CAG-GFP	Salk Viral Vector Core Facility	N/A
AAV9.CamKII0.4.Cre.SV40	Penn vector core	AV-9-PV2396
Cre-dependent HSV-H129ΔTK-tdTomato	Lo and Anderson, 2011	N/A
Experimental Models: Cell Lines		
NSI-566RSC-GFP	NeuralStem, Inc	N/A
Experimental Models: Organisms/Strains		
Rat: Fisher 344 (F344/NHsd)	Envigo	N/A
Rhesus macaques (Macaca mulatta)	Rosenzweig et al., 2018	N/A